September 9, 2010

Silver nanosphere SERS probes for sensitive identification of pathogens

Kyuwan Lee, *University of California - Berkeley*

Silver Nanosphere SERS Probes for Sensitive Identification of Pathogens

Yuling Wang, Kyuwan Lee, and Joseph Irudayaraj*

Physiological Sensing Facility, Bindley Bioscience Center and Birck Nanotechnology Center, Purdue University, 225 South University Street, 215 ABE Building, West Lafayette, Indiana 47907

Received: February 20, 2010; Revised Manuscript Received: August 19, 2010

The identification and timely detection of pathogenic bacteria is critical to ensuring safe food, health, and water. Although surface enhanced Raman scattering (SERS) methods have been used for pathogen characterization and single molecule sensing, the challenge of detecting pathogens in very low numbers using an optimal substrate that is sensitive and reproducible is still a challenge. In this report, we have developed and explored a novel SERS active substrate of 60−80 nm diameter through the assembly of Ag nanocrystals (AgNCs) into Ag nanospheres (AgNSs). A finite difference time domain (FDTD) analysis of the electromagnetic field produced by these structures and the enhancement factor calculations indicated that an enhancement of 10^8 was possible using the 633 or 785 nm excitation. The exact enhancement factors (EF) through the experimental results were calculated to be 2.47×10^7, which is close to that obtained through the FDTD analysis. Preliminary characterization of the SERS substrate was demonstrated using various labels from the fluorescent dye and nonfluorescent small molecules. More importantly, these novel SERS active substrates when used for pathogenic bacteria detection could detect cells as few as 10 colony forming units/mL (CFU/mL). Using canonical variate analysis (CVA) in conjunction with Raman spectra, differentiation of three key pathogens (*E. coli* O157, *S. typhimurium*, and *S. aureus*) including live and dead cells was also accomplished. With further optimization of the SERS substrate, single cell detection is possible.

Introduction

The identification and timely detection of pathogenic bacteria in food is critical because many serious and even fatal medical conditions result from bacterial infection or contamination. Pathogens are of significant concern to not only food safety but also to recipients of blood transfusions.[1] Reports indicate that 1.5 billion people around the world are infected by bacteria each year. The cost of preventive and curative measures to combat pathogen infection/contamination is estimated to be ∼$6.9 billion annually, according to the Economic Research Service (ERS) in 2000.[2] Traditional methods used for pathogen detection involve the basic steps of pre-enrichment, selective enrichment, biochemical screening, and serological confirmation, which are selective and specific, but, because they rely on a series of enrichment steps, the results are often difficult to interpret and not available in the time scale desired for quick remedial measures to be undertaken.[3] A number of methods have been developed, including flow cytometry,[4] PCR,[5] and ELISA,[6] among other standard molecular biology-based assays. However, rapid detection of a low number of cells (<10 CFU/ML) is still a challenge.

It has been shown that Raman scattering can provide rich structural and qualitative and quantative information of analytes in their physiological state through their sharp and distinguishable vibrational bands of functional groups. Conventional Raman spectroscopy is not sensitive and in most cases requires a large collection time, potentially resulting in damage to the sample. Since the advent of surface enhanced Raman scattering (SERS) in the 1970s,[7] SERS applications in biological systems have increased especially because of their exquisite sensitivity to detect even single molecules due to the huge enhancement.[8]

Two enhancement mechanisms relating to Raman scattering can be construed, the charge transfer mechanism[9] and the electromagnetic mechanism (EM).[10] According to the EM model, a large enhancement is possible when the gap between nanoparticles is less than 10 nm, depicted by hot spots (highly localized regions of large local field enhancement).[11] Although this theory is not conclusive, hot spots can be generated in structures fabricated using lithographic and template methods.[12] Recently, the bottom-up assembly using small nanocrystals as building blocks has attracted tremendous attention[13] because of the lower cost of synthesis protocols. Structures obtained through this route have been used in catalysis,[14] biomedical diagnosis,[15] and high-density data storage.[16] However, only few studies have used nanospheres constructed from the bottom-up assembly as SERS substrates.

Compared to other technologies used for pathogen detection, such as PCR,[17a] Fourier transform infrared spectroscopy,[17b] and, more recently, mass spectrometry,[17c] SERS has been shown to be a useful and powerful tool in pathogen identification and discrimination because of its ability to generate whole organism fingerprints[17d–f] with high speed and great specificity and, more importantly, the relative ease of experimental implementation. To a large extent, silver and gold nanoparticles of various shapes and sizes or even aggregates induced by inorganic salt have been used as SERS substrates,[18] but these substrates have poor reproducibility due to the challenge posed by efficient control of the aggregation process. Successful detection by SERS is possible if the substrates fabricated are reproducible and provide sufficient enhancement to detect single cells.

A bottom-up assembly of silver nanocrystals (AgNCs) to form silver nanospheres (AgNSs) as SERS substrate with hot spots was accomplished in this work by using small AgNCs as building blocks in a microemulsion of oil droplets within which AgNCs are assembled into AgNSs by the evaporation of low boiling point solvents. Due to the significant electromagnetic coupling effect between small AgNCs in the nanospheres, an enhancement factor as high as 10^8 was possible, as demonstrated

10.1021/jp1015406
Published on Web 09/09/2010

by finite difference time domain (FDTD) simulation and the exact enhancement factor calculated according to the experimental spectra. Because these hot spots could be distributed around these AgNSs, we hypothesize that a reproducible enhanced signal is possible. In this report we further demonstrate the use of these highly sensitive SERS-active substrates to identify, classify, and characterize key pathogens of interest to food safety and biosecurity.

Experimental Section

Materials. Silver nitrate (99%), sodium oleate, oleic acid, sodium dodecyl sulfate (SDS), 4-mercaptobenzoic acid (MBA), *trans*-1,2-bis(4-pyridyl) ethylene (BPE), and rhodamine B isothiocyanate (RITC) were all purchased from Sigma-Aldrich. Milli-Q grade water was used in experiments.

Preparation of AgNCs. AgNCs were prepared with minor modifications to the proposed protocol.[19] Briefly, 1 g $AgNO_3$, 20 mL of deionized water, 1.6 g sodium oleate, 2 mL of oleic acid, and 10 mL of ethanol were added into a 50 mL autoclave tube sequentially. The system was sealed and treated at 150 °C for 24 h. After reaction, the product was washed three times with ethanol and then dried to obtain a solid sample.

Preparation of Water-Dispersed AgNSs from Oil-Dispersed AgNCs. SDS (28 mg) was added to deionized water (5 mL). A solution containing AgNCs (4 mg) in cyclohexane (1 mL) was added to the SDS aqueous solution, and the system was emulsified by ultrasonic treatment for 60 min. The cyclohexane was removed by heating at 70 °C to assemble the NCs into AgNSs.[20] After the reaction was cooled to room temperature, the products were collected and purified by repeated centrifugation and redispersed in water.

Preparation of Bacteria Samples. Bacteria (*Staphylococcus aureus*, *E. coli* O157:H7#99.0874, *E. coli* O157:H7#5.2262, and *S. typhimurium*) were grown in Luria-Bertini broth at 37 °C and collected with sterile plastic innoculating loops from solid culture plates. Samples were then collected after the bacteria were cultured for 13 h with shaking for all experiments. The collected samples were added to 3 mL of PBS (pH 7.4), vortexed, and centrifuged for 10 min at 5800 rpm and the supernatant was then discarded. The procedure was repeated three times.

Measurement. The size and morphology of AgNCs and AgNSs were determined by transmission electron microscopy (TEM), acquired with a Philips CM-100 TEM (Philips, Eindhoven, Netherlands) operating at 100 kV. SEM images of AgNSs were obtained with a Zeiss DSM 982 Gemini instrument.

Absorption spectra of AgNCs in cyclohexene and AgNSs in water were measured with a Jasco V570 UV/visible/NIR spectrophotometer (Jasco, Inc., Easton, MD) in the 400 and 900 nm wavelength range.

SERS measurements of the Raman labels on AgNSs for enhancement characterization were conducted using the SENTERRA confocal Raman system (Bruker Optics Inc., Billerica, MA) with a 20× air objective at 633 and 785 nm excitation, respectively. The laser power and accumulation time were 20 mW and 10 s at 633 nm and 10 mW and 10 s at 785 nm excitation, respectively. A 50 μm pinhole was used for confocality.

SERS spectra of bacteria incubated with AgNSs for 30 min were acquired with a 5 s integration time using a 100 × objective with a 785 nm excitation at 1 mW laser power. The initial concentration was obtained by plate count and serially diluted from there on.

Finite Difference Time Domain (FDTD) Simulation. A commercial FDTD software package (RemCom XFDTD 6.2, State college, PA) employing the modified Debye model[21] with the boundaries of Liao's absorption conditions[22] was used for simulating the electromagnetic field enhancement in the vicinity of the nanoparticle structure in vacuum. Silver nanocrystals of size 13 nm and 1−2 nm spacing were used to form the SERS nanospheres of size 60−80 nm.

Data Analysis. Classification of different bacterial species was carried out using canonical variate analysis (CVA) based on the Raman spectra. The Win-DAS (Wiley, Chichester, U.K.) software package developed by Kemsley was used to differentiate bacteria.[23] Before analysis, area normalization and baseline correction of the spectra were employed to eliminate unwanted instrumental effects on the data set. Principal component analysis (PCA) was used to compress the data to a manageable size prior to discriminated analysis.

Results and Discussion

Figure 1A summarizes the assembly of AgNCs into AgNSs for pathogen detection. AgNCs were first prepared according to the method reported by Wang et al.[19] To obtain small nanocrystals with uniform size distribution, the reaction temperature and time was optimized to provide uniform small AgNCs at 150 °C with a 24 h reaction time. The nanocrystals were then assembled through spontaneous attraction by the hydrophobic van der Waals interaction of the surfactant ligands (SDS) absorbed onto the AgNCs during controlled evaporation of cyclohexane in the restricted, nanometer-sized three-dimensional configuration provided by the microemulsion droplets.[20] After an ultrasonication step, stable AgNSs with good solubility in water were obtained. For detection, the SERS substrate was mixed with bacteria, as shown in the scheme of Figure 1A and taken for Raman measurements.

To begin with, we first investigate the morphology and optical properties of AgNCs and AgNSs. A representative TEM image of the as-prepared AgNCs is shown in Figure 1B, and the high magnification inset shows that the clusters are uniform with a diameter of ∼13 nm. UV−vis absorption spectrum of AgNCs in Figure 1D (curve a) shows a very narrow and sharp peak at 409 nm, demonstrating that AgNCs with regular sizes can be used as building blocks for successful assembly into AgNSs. Inset optical images in Figure 1D clearly show the AgNCs dispersed on top of the oil phase. However, after assembly, the AgNSs show excellent dispersibility in the aqueous phase. SEM and TEM images of the as-prepared AgNSs (Figure 1C) indicate the diameter to be in the range 60−80 nm, and contain holes, junctions, and crevices conducive for significant enhancement.[24] Further, it is known that gap structures on metal surface can support a strong localized electromagnetic field for SERS, which can induce a giant enhancement of the dipole moment of the analyte.[25] Therefore, significant localized electromagnetic field of the target in the proximity of AgNSs is possible because of the large electromagnetic coupling effect provided by the gaps between the AgNCs that form into AgNSs. Curve b in Figure 1D gives the UV−vis absorption spectrum of AgNSs at 425 nm, which is broader than that of AgNCs, indicative of the assembly state of the nanocrystal.[26]

To evaluate the enhancement effect of the as-prepared AgNSs as SERS probes, two different small molecules (MBA and BPE) at a concentration of 10^{-5} M and a dye molecule (RITC) at a concentration of 10^{-7} M were used for evaluation at the red (633 nm) and near-infrared (785 nm) excitations. Red and near-infrared laser excitations were chosen because

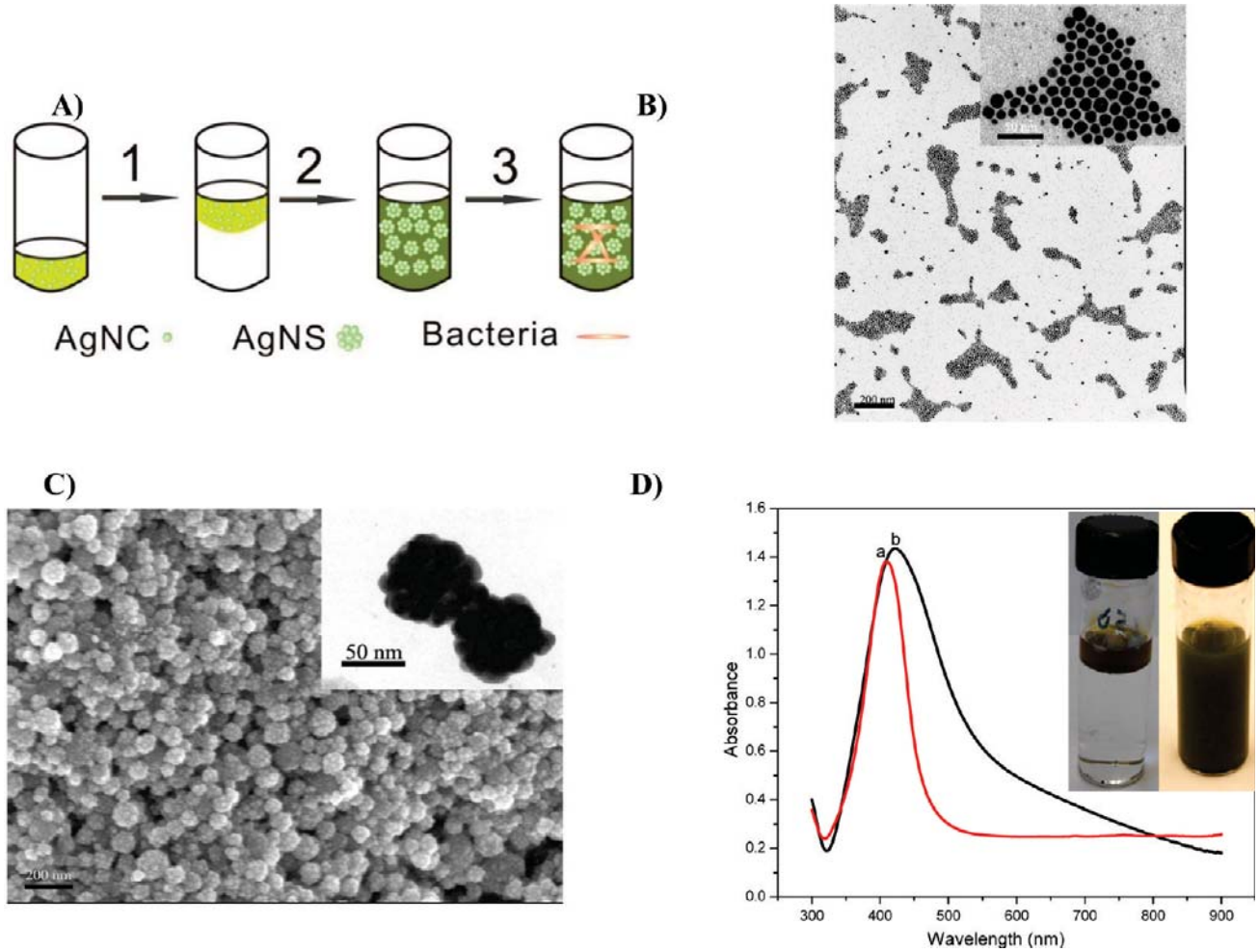

Figure 1. (A) Schematic of the formation of SERS active AgNSs substrate for pathogen detection: (1) SDS aqueous solution; (2) sonication for 60 min and evaporation of cyclohexane at 70 °C; (3) pathogenic bacteria detection. (B) Typical TEM image of AgNCs in a large scale and the inset shows the highly magnified image of AgNCs. (C) Typical SEM image of the as-prepared AgNSs (inset is the typical TEM image of AgNSs). (D) UV−vis absorption spectra of AgNCs in cyclohexene (curve a) and AgNSs in aqueous phase (curve b). Inset is the optical photograph of AgNCs in a mixture of oil and water phase (left) and AgNSs in the aqueous phase (right).

this spectral region is known to provide a clear window for optical imaging with minimal interference from water.[27] Raman measurement (with a 633 nm excitation) of two of the Raman reporters (MBA and RITC) on the 13 nm AgNCs dried on a glass substrate show that only a weak signal is possible because of the suboptimal size of nanoclusters for enhanced Raman experiments (spectrum b and c in Figure S1). Cyclohexane (spectrum a from Figure S1) was used to obtain monodispersed AgNCs, as they do not easily dissolve in water. Only a weak Raman signal was possible because of the small size and the surface characteristics of silver particles. Figure 2 shows the SERS spectra of these probes on AgNSs at 633 and 785 nm excitation, respectively. First, a weak signal on the blank AgNSs (spectrum a) was obtained to assess the background and interference during detection. It should be noted that the SDS around AgNSs, could produce only a very weak signal because of the small cross section of SDS, which will not interfere with the detection for the target molecules. Next, spectra of these small molecules were obtained both at 633 and 785 nm excitation. Characteristic vibrational bands of MBA at 1586, 1078, 1379, and 1180 cm^{-1}, assigned to the ν_{8a} and ν_{12} aromatic ring vibrations and νcoo- and δcoo-, respectively, were observed.[28] Strong SERS peaks of BPE located at 1013, 1204, 1337, 1611, and 1640 cm^{-1}, assigned to the ethylenic C═C stretch; C−H bending on the pyridine ring, C═C stretching mode, aromatic ring stretching mode and in-plane aromatic ring modes[29] were also observed.

Comparison of SERS spectra of MBA on citrate-reduced silver nanoparticles (AgNPs) and AgNSs of comparable size (TEM image of citrate-AgNPs is shown in Figure S2A and spectra in Figure S2B) shows that SERS signal obtained from AgNSs is 3−4 times greater than that obtained from citrate-AgNPs. The high enhancement is ascribed to the fact that AgNSs can provide a giant electromagnetic field due to the crevices, holes, and junctions of the assembled AgNCs on AgNSs. To further demonstrate the large electromagnetic field produced on AgNSs, FDTD simulation for the electromagnetic field on the nanostructures was examined and presented in Figure 3. The size of AgNCs (Figure 3A) used in the simulation was 13 nm at an interparticle spacing of 1−2 nm to produce spheres of 60−80 nm in size. The local electromagnetic fields when excited by a 785 nm laser show a maximum enhancement of $\sim 10^8$ between nanoparticles (Figure 3B), sufficient to generate a detectable Raman signal of small numbers of molecules in the enhancement field.[30] Such high enhancements are not possible from an isolated single nanoparticle regardless of its size, which is in agreement with theory.[31] Furthermore, as reported by Kneipp et al, enhancement factors for isolated silver nanoparticles

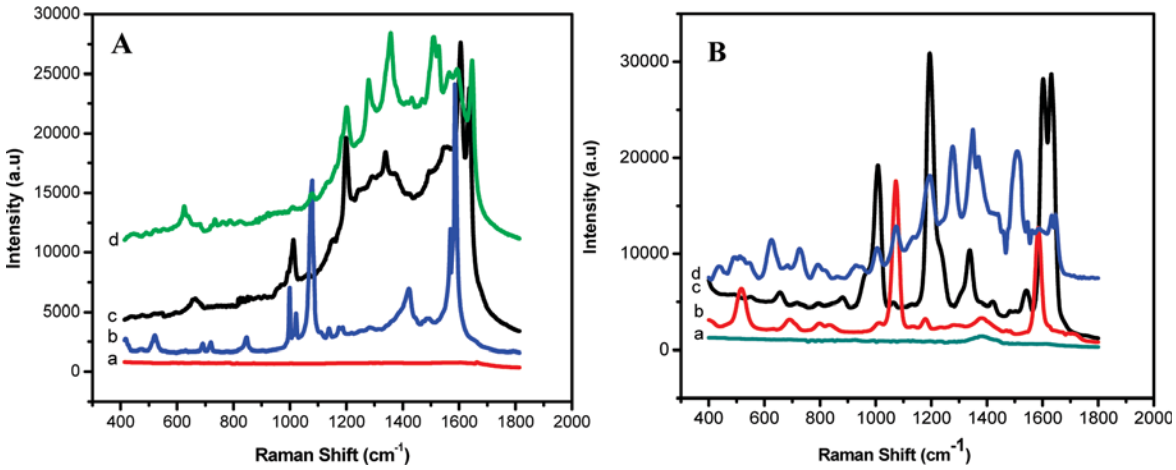

Figure 2. Raman spectra of blank AgNSs (a) and SERS spectra of labels, MBA, BPE, and RITC (b−d) on the as-prepared AgNSs at 633 (A) and 785 nm (B) excitations, respectively.

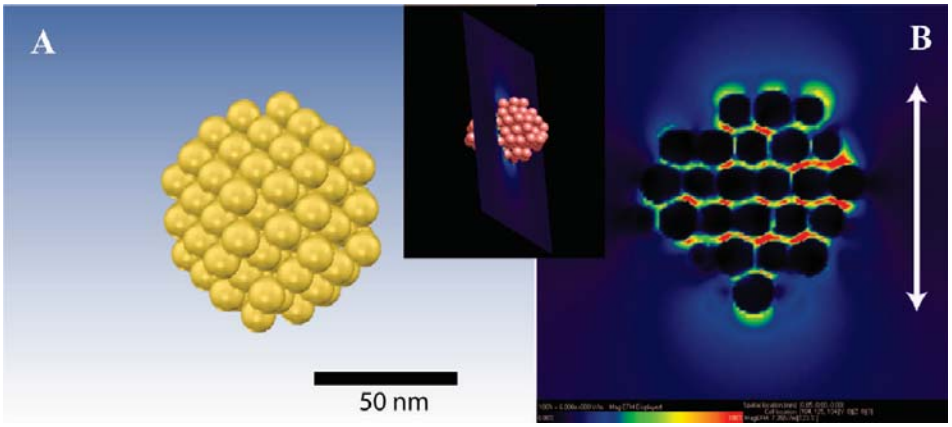

Figure 3. Electromagnetic near field enhancement simulated by FDTD method with a 785 nm laser excitation. Original model (A) is simulated and near field enhancement in the typical slice of cross-section (inset) is presented (B).

are estimated to be 7 orders of magnitude lower than the enhancement factor for nanoparticles with junctions (enhancement factor as high as 10^{10} has been reported),[32] indicating that the localized plasmon at the junctions between adjacent nanoparticles will give rise to very large electromagnetic field enhancement.[33] Higher enhancement from isolated clusters, called hot particles[34] has also been reported, but reproducible of this enhancement field is highly inconsistent. Past theoretical[35] and experimental[36] studies also indicate that such high enhancement cannot be reached by increasing the size of the nanoparticle because the resonance peak shift of silver nanoparticles depends to a greater extent on the type of material. Interestingly, while the average enhancement by the 633 nm excitation was 5−10 times higher than the 785 nm excitation (shown in Figure S3), the maximum enhancement by both excitations were close to each other because of the strong interaction between the local structures (hot spot), which are not necessarily coupled with the excitation wavelength demonstrated previously.[36] Meanwhile, the enhancement factor from the AgNSs and the citrate-AgNPs of similar size and shape were also compared using FDTD simulation (as shown in the Supporting Information, Figure S3C).[37] Results show that the enhancement factor obtained from AgNPs is approximately 10^4∼10^5, 2−3 orders of magnitude lower than that obtained from AgNSs, clearly showing that large enhancements are possible due to the surface characteristics of AgNSs. The enhancement factor (EF) were calculated according to the following equation[38] using the experimental data,

$$\mathrm{EF} = \frac{I_{\mathrm{SERS}}/N_{\mathrm{ads}}}{I_{\mathrm{bulk}}/N_{\mathrm{bulk}}}$$

where I_{SERS} and I_{bulk}, respectively, denote the intensity of a vibrational mode in the SERS and normal spectrum. The vibrational peak of C−S bond (at 1078 cm^{-1} in SERS spectra and 1094 cm^{-1} in normal Raman spectrum) in MBA was chosen to calculate the EF value. N_{ads} and N_{bulk} denote the number of MBA molecules adsorbed on the substrate and bulk molecules illuminated by the laser light. N_{ads} can be obtained according to the method proposed by Orendorff et al.[28b] from

$$N_{\mathrm{ads}} = N_{\mathrm{d}} \cdot A_{\mathrm{laser}} \cdot \mathrm{AN}/\sigma$$

where N_{d} is the number density of the nanoparticles, A_{laser} is the area of the focal spot of laser, A_{N} is the footprint area of nanoparticles and σ is the surface area occupied by an adsorbed MBA molecule. Here the total number of surface adsorbed molecules within the illuminated laser spot (N_{ads}) was estimated as 7.85×10^6, and N_{bulk} was calculated to be about 1.42×10^{12}. Considering the intensity ratio of the C−S

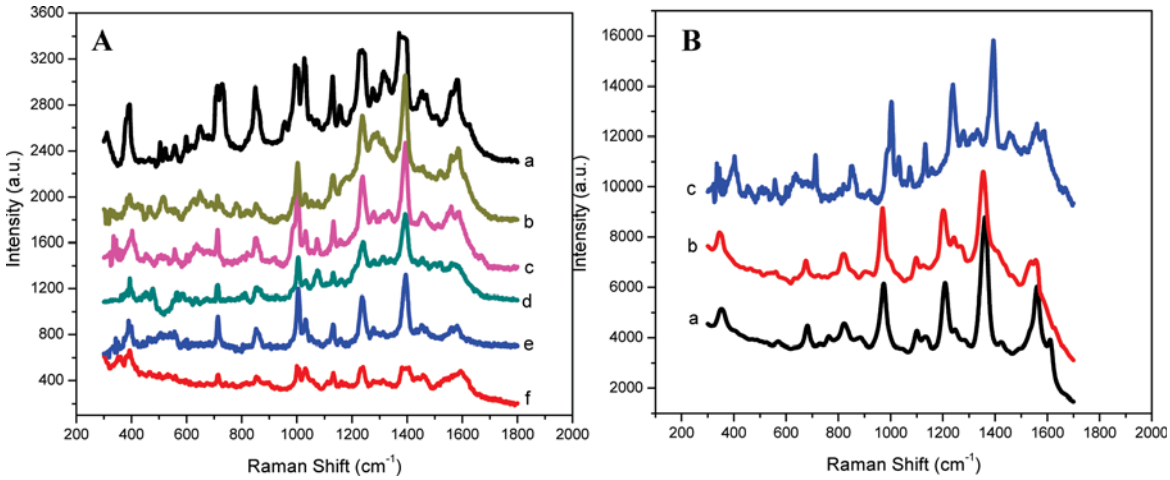

Figure 4. (A) SERS spectra of *S. aureus* on the as-prepared AgNSs at concentrations of a, 10^6; b, 10^5; c, 10^4; d, 10^3; e, 10^2; and f, 10 CFU/mL. (B) Comparison of SERS spectra of *E. coli* O157 (a), *S. typhimurium* (b), and *S. aureus* (c) at 785 nm excitation.

TABLE 1: Tentative Assignment of Peaks from the SERS Spectra of *E. coli* O157: H7, *S. typhimurium*, and *S. aureus*[a]

E. coli O157:H7	*S. typhimurium*	*S. aureus*	
Raman shift (cm^{-1})			assignment
570	564	555	carbohydrates
		634	COO^- bend
680	678	712	adenine
761			ring I deformation
823	817	850	different C−N stretch
890	904	918	
974	968	1003	C═C deformation
		1032	
1099	1099	1073	carbohydrates, C−C, C−O, −C−OH
1131	1125	1131	deformation
		1157	═C−C═ unsaturated fatty acids in lipids, C−N
1209	1204		aromatic amino acids in proteins
1244	1244	1238	
	1276	1285	amide III
1361	1355	1334	═CH in plane (lipid) or amide III (protein)
		1395	adenine, guanine (protein) C−H deformation
		1453	COO^- stretching
1558	1552	1558	CH_2 deformation
1614	1628	1594	adenine, guanine (ring stretching)

[a] Obtained from refs 39a and 40.

peak in SERS and Normal mode (calculated to be 13.7, normalized with respect to the absolute intensity of a silicon wafer), the EF of AgNSs was estimated to be about 2.47×10^7, which is close to the value obtained from our FDTD simulation. The high enhancement of these evaluator molecules due to the AgNSs makes these structures an ideal candidate for developing highly sensitive SERS platforms.[39]

As a next step, three different species of bacteria were chosen as test organisms and their Raman fingerprint were recorded (Figure 4). Concentration-based spectra (Figure 4A) of *S. Aureus* (a gram-positive bacterium) show the typical Raman bands of adenine, amine, membrane proteins, phospholipids, and polysaccharides consistent with the literature.[39a,40] With the 785 nm excitation, the enhancement provided by the AgNSs allowed the observation of Raman spectra of *S. aureus* at a concentration as low as 10 CFU/mL at an incident powers of 1 mW with a 5 s acquisition time. Characteristic Raman fingerprint of the pathogen was possible even at this low concentration (Figure 4A). Comparison of SERS signals of pathogens (10^4 CFU/mL) on AgNSs with that of AgNPs of the same size and similar experimental conditions shown[39b] in Figure S4 indicates that the signal from AgNPs was significantly weaker. Significant enhancement from AgNSs is possible due to its surface characteristics which could comprise of crevices and gap junctions within each monodispersed entity, contributing an electromagnetic field which is 2−3 orders of magnitude larger than the citrate-AgNPs as shown by simulation (Figure S3) as well as from the spectra in Figures S1 and S2.

To further demonstrate the versatility of the SERS substrate, two types of gram-negative bacteria were tested at the concentration of 10^2 CFU/mL and distinct SERS spectra of *S. typhiumuirm* and *E. coli* O157:H7 were recorded (Figure 4B). Compared to the SERS spectra of *S. aureus*, they share many common spectra features, however, clear differences in the vibration bands and the relative intensity exists. Table 1 gives the Raman shift and tentative band assignment of the SERS spectra of three different bacterial species. We expect these unique SERS vibrational signatures to provide the basis for a rapid pathogen identification methodology development when combined Chemometrics.[25a] Figure 5 shows the CV2 versus CV1 plot from canonical variate analysis (CVA) using a 25 spectra data set, respectively, from the three bacterial species. The SERS signal of *E. coli* O157:H7, *S. typhimurium*, and *S. aureus* are well-separated and nonoverlapping from the CVA

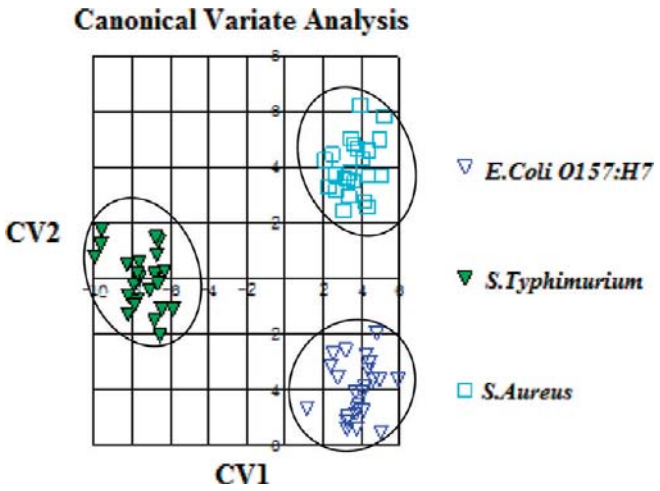

Figure 5. Canonical variate analysis of the SERS spectra of three pathogens, *E. coli* O157, *S. typhiumium*, and *S. aureus*.

analysis, a multivariate statistical analysis procedure used for classification.

To test for the reproducibility of SERS detection, six replicative spectra of two different bacteria were collected from six different samples. Typical SERS spectra shown in Figure S5 indicate excellent similarity between this replicates.[17c] Different *E. coli* O157:H7 isolates of human origin were also distinguished by SERS as shown in Figure S4A and B, respectively. Distinct SERS spectra of *E. coli* O157:H7#5.2262 and *E. coli* O157:H7#99.0874 was also possible. Although they share similar characteristic peaks, the relative band widths and intensities were somewhat different. Clear separation was observed (Figure S6) between these isolates (100 CFU/mL) using CVA. It should be noted that excellent reproducibility of Raman signal from pathogens was possible from the AgNSs. Assuming a length of 2−3 μm and a width of 0.6−0.9 μm for a bacterium, approximately 8.25 $\times$ 10^2 AgNSs (80 nm in diameter) could be present per cell. Because the laser spot size has a diameter of 1 μm, we expect a maximum of 3.24 $\times$ 10^2 monodispersed AgNSs to be present in the laser focal volume and contribute to the enhancement.

In addition to detection and differentiation of live bacteria, the versatility of these novel AgNSs SERS substrates was also demonstrated (Figure 6) in distinguishing between live and dead species, a critical area in food safety. The bacteria were first killed by autoclaving at 120 °C for 10 min. A considerable difference in the spectra of dead and live cells were obtained possibly due to the rupture of the outer layer of the bacterial cell wall with a possible change in the membrane proteins resulting in the release of carbohydrates from these cells.[41] All of these changes contribute to inducing a significant difference in the SERS signal between the live and dead samples. CVA shows a clear separation between the live and dead bacteria (Figure S7) even at a concentration as low as 10^3CFU/mL.

Conclusions

In summary, we have developed and explored a novel monodispersed AgNSs SERS substrate formed by the assembly of AgNCs through a bottom-up assembly for sensitive detection of multiple pathogens. Due to the large electromagnetic coupling between the AgNCs that form AgNSs, enormous enhancement was possible due to the enhanced Raman scattering of the target analytes at the red and near-infrared excitations. A FDTD analysis of the electromagnetic field produced by these structures and the enhancement factor calculations indicated that an enhancement factor of $\sim 10^8$ was possible using the 633 or 785 nm excitation. More importantly, the synthesized SERS substrate was used to detect bacteria at a concentration as low as 10 CFU/mL with excellent signal reproducibility. Classification of the three key pathogens as well as live and dead bacteria was also accomplished. Based on the results, with further refinement and optimization of the SERS substrate, we expect that AgNSs could be designed to detect a single pathogen.

Acknowledgment. This research was partly supported by the Center for Food Safety Engineering Grant 1935-42000-035, USDA−Purdue University. Sandeep Ravindranath is acknowledged for his assistance in culturing bacteria. Pathogenic strains were obtained from Dr. Chobi Debroy from The Pennsylvania State University, University Park, PA.

Supporting Information Available: Raman spectrum of AgNCs in cyclohexane and SERS spectra of Raman reporters (MBA and RITC); TEM image of citrate-AgNPs and SERS spectra of MBA on citrate-AgNPs, AgNSs were given; Comparison of the electromagnetic field on AgNSs at 633 and 785

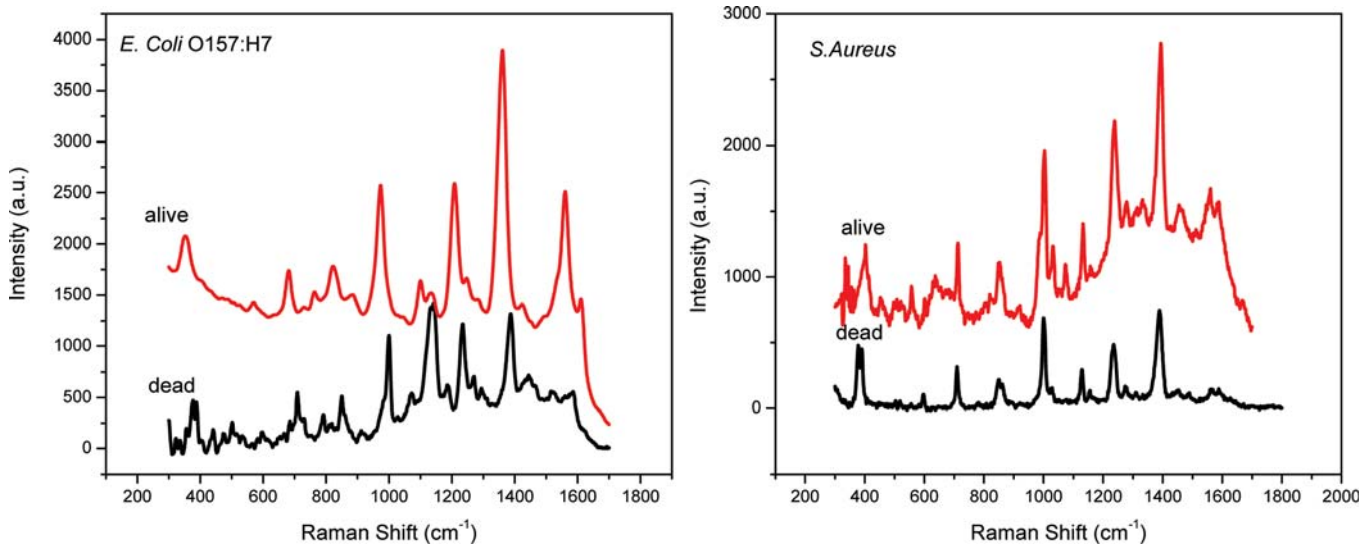

Figure 6. Comparison of SERS spectra of live and dead bacteria at a concentration of 10^2 CFU/mL.

nm exciation; SERS spectra of *E. coli* O157:H7#5.2262 and *E. coli* O157:H7#99.0874; CVA of SERS spectra of different *E. coli* O157:H7 isolates of human origin and SERS spectra of live and dead bacteria (*E. coli* O157:H7#5.2262). This material is available free of charge via the Internet at http://pubs.acs.org.

References and Notes

(1) Mead, P. S.; Slutsker, L.; Dietz, V. *Emerging Infect. Dis.* **1999**, *5*, 607.

(2) ERS. http://ers.usda.gov/briefing/foodbornedisease (accessed Sept. 23, 2003).

(3) Maalouf, R.; Fournier-Wirth, C.; Coste, J.; Chebib, H.; Saǩali, Y.; Vittori, O.; Errachid, A.; Cloarec, J. P.; Martelet, C.; Jaffrezic-Renault, N. *Anal. Chem.* **2007**, *79*, 4879.

(4) (a) Hibi, K.; Abe, A.; Ohashi, E.; Mitsubayashi, K.; Ushio, H.; Hayashi, T.; Ren, H.; Endo, H. *Anal. Chim. Acta* **2006**, *173*−*174*, 158. (b) Kempf, V. A. J.; Mändle, T.; Schumacher, U.; Schäfer, A.; Autenrieth, I. B. *Int. J. Med. Microbiol.* **2005**, *295*, 47.

(5) (a) Hoshino, T.; Kawaguchi, M.; Shimizu, N.; Hoshino, N.; Ooshima, T.; Fujiwara, T. *Diagn. Microbiol. Infect. Dis.* **2004**, *8*, 195. (b) Lazaro, D. R.; Hernandez, M.; Esteve, R.; Hoofar, J.; Pla, M. *J. Microbiol. Methods* **2003**, *54*, 381. (c) Greisen, K.; Loeffelholz, M.; Purohit, A.; Leong, D. *J. Clin. Microbiol.* **1994**, *32*, 335.

(6) (a) Bryniok, D.; Trösch, W. *Appl. Microbiol. Biotechnol.* **1989**, *32*, 235. (b) Sandström, G. E.; Wolf-Watz, H.; Tärnvik, A. *J. Microbiol. Methods* **1986**, *5*, 41. (c) Dylla, B. L.; Vetter, E. A.; Hughes, J. G.; Cockerill, F. R. *J. Clin. Microbiol.* **1995**, *33*, 222.

(7) (a) Fleischmann, M.; Hendra, P. J.; McQuillan, A. J. *Chem. Phys. Lett.* **1974**, *26*, 163. (b) Jeanmaire, D. L.; Van Duyne, R. P. *J. Electroanal. Chem.* **1977**, *84*, 1. (c) Albrecht, M. G.; Creighton, J. A. *J. Am. Chem. Soc.* **1977**, *99*, 5215.

(8) (a) Nie, S. M.; Emory, S. R. *Science* **1997**, *275*, 1102. (b) Kneipp, K.; Wang, Y.; Kneipp, H.; Perelman, L. T.; Itzkan, I.; Dasari, R. R.; Feld, M. S. *Phys. Rev. Lett.* **1997**, *78*, 1667.

(9) (a) Otto, A.; Billmann, J.; Eickmans, J.; Erturk, U.; Pettenkofer, C. *Surf. Sci.* **1984**, *138*, 319. (b) Arenas, J. F.; Woolley, M. S.; Otero, J. C.; Marcos, J. I. *J. Phys. Chem.* **1996**, *100*, 3199.

(10) (a) Kahl, M.; Voges, E. *Phys. Rev. B* **2000**, *61*, 14078. (b) Shalaev, V. M.; Sarychev, A. K. *Phys. Rev. B* **1998**, *57*, 13265. (c) Moskovits, M.; Dilella, D. P.; Maynard, K. L. *Langmuir* **1988**, *4*, 67.

(11) (a) Vosgröne, T.; Meixner, A. J. *ChemPhysChem* **2005**, *6*, 154. (b) Li, W. Y.; Camargo, P. H. C.; Lu, X. M.; Xia, Y. N. *Nano Lett.* **2009**, *9*, 485.

(12) (a) Wang, H.; Levin, C. J.; Halas, N. J. *J. Am. Chem. Soc.* **2005**, *127*, 14992. (b) Wang, H.; Liu, C.; Wu, S.; Liu, N.; Peng, C.; Chan, T.; Hsu, C.; Wang, J.; Wang, Y. *Adv. Mater.* **2006**, *18*, 491. (c) Braun, G.; Pavel, I.; Morrill, A. R.; Seferos, D. S.; Bazan, G. C.; Reich, N. O.; Moskovits, M. *J. Am. Chem. Soc.* **2007**, *129*, 7760.

(13) (a) Zhuang, J. Q.; Wu, H. M.; Yang, Y.; Cao, Y. C. *J. Am. Chem. Soc.* **2007**, *129*, 14166. (b) Wang, D. S.; Xie, T.; Peng, Q.; Li, Y. D. *J. Am. Chem. Soc.* **2008**, *130*, 4016.

(14) Somorjai, G. A.; Rioux, R. M.; Grunes, J. In *Clusters and Nano-Assemblies*; Jena, P., Khanna, S. N., Rao, B. K., Eds.; World Scientific Publishing: NJ, 2005; pp 97−125.

(15) (a) Mirkin, C. A.; Letsinger, R. L.; Mucic, R. C.; Storhoff, J. J. *Nature* **1996**, *382*, 607. (b) Han, M.; Gao, X.; Su, J. Z.; Nie, S. *Nat. Biotechnol.* **2001**, *19*, 631.

(16) Sun, S.; Murray, C. B.; Weller, D.; Folks, L.; Moser, A. *Science* **2000**, *287*, 1989.

(17) (a) Belgrader, P.; Benett, W.; Hadley, D.; Richards, J.; Stratton, P.; Mariella, R., Jr.; Milanovich, F. *Science* **1999**, *284*, 449. (b) Naumann, D.; Helm, D.; Labischinski, H. *Nature* **1991**, *351*, 81. (c) Lay, J. O. J. *Trends Anal. Chem.* **2000**, *19*, 507. (d) Jarvis, R. M.; Goodacre, R. *Anal. Chem.* **2004**, *76*, 40. (e) Jarvis, R. M.; Brooker, A.; Goodacre, R. *Faraday Discuss.* **2006**, *132*, 281. (f) Jarvis, R. M.; Brooker, A.; Goodacre, R. *Anal. Chem.* **2004**, *76*, 5198.

(18) (a) Premasiri, W. R.; Moir, D. T.; Klempner, M. S.; Krieger, N.; Jones, G.; Ziegler, L. D. *J. Phys. Chem. B* **2005**, *109*, 312. (b) Zeiri, L.; Bronk, B. V.; Shabtai, Y.; Czégé, J.; Frima, S. *Colloids Surf., A* **2002**, *208*, 357. (c) Sengupta, A.; Laucks, M. L.; Davis, E. J. *Appl. Spectrosc.* **2005**, *59*, 1016. (d) Laucks, M. L.; Sengupta, A.; Junge, K.; Davis, E. J.; Swanson, B. D. *Appl. Spectrosc.* **2005**, *59*, 1222.

(19) Wang, X.; Zhuang, J.; Peng, Q.; Li, Y. D. *Nature* **2005**, *437*, 121.

(20) (a) Bai, F.; Wang, D. S.; Huo, Z. Y.; Chen, W.; Liu, L. P.; Liang, X.; Chen, C.; Wang, X.; Peng, Q.; Li, Y. D. *Angew. Chem., Int. Ed.* **2007**, *46*, 6650. (b) Zhuang, J.; Wu, H.; Yang, Y.; Cao, Y. C. *J. Am. Chem. Soc.* **2007**, *129*, 14166.

(21) Kunz, K. S.; Luebbers, R. J. *The Finite Difference Time Domain Method for Electromagnetics*; CRC Press: New York, 1993.

(22) Liao, Z. P.; Wong, H. L.; Yang, B. P.; Yuan, Y. F. *Sci. Sin.* **1984**, *27* (10), 1063–1076.

(23) Kemsley, E. K. *Discriminant Analysis and Class Modeling of Spectroscopic Data*; John Wiley & Sons Ltd.: Chichester, 1998; pp 111−115.

(24) (a) Krug, J. T.; Wang, G. D.; Emory, S. R.; Nie, S. M. *J. Am. Chem. Soc.* **1999**, *121*, 9208. (b) Qian, X.; Peng, X. H.; Ansari, D. O.; Goen, Q. Y.; Chen, G. Z.; Shin, D. M.; Yang, L.; Young, A. N.; Wang, M. D.; Nie, S. *Nat. Biotechnol.* **2008**, *26*, 83.

(25) (a) Yan, B.; Thubagere, A.; Premasiri, W. R.; Ziegler, L. D.; Negro, L. D.; Reinhard, B. M. *ACS Nano* **2009**, *3*, 1190. (b) Moskovits, M. *Rev. Mod. Phys.* **1985**, *57*, 783.

(26) (a) Wang, Y. L.; Zou, X. Q.; Ren, W.; Wang, W. D.; Wang, E. K. *J. Phys. Chem. C* **2007**, *111*, 3259. (b) Rendell, R. W.; Scalapino, D. J. *Phys. Rev. B* **1981**, *24*, 3276.

(27) Mahmood, U.; Weissleder, R. *Mol. Cancer Ther.* **2003**, *2*, 489.

(28) (a) Xu, S.; Ji, X.; W., Xu; Li, X.; Wang, L.; Bai, Y.; Zhao, B.; Ozaki, Y. *Analyst* **2004**, *129*, 63. (b) Orendorff, C. J.; Gole, A.; Sau, T. K.; Murphy, C. *J. Anal. Chem.* **2005**, *77*, 3261.

(29) (a) Yang, W. H.; Hulteen, J. C.; Schatz, G. C.; Van Duyne, R. P. *J. Chem. Phys.* **1996**, *104*, 4313. (b) Liu, Y.; Fan, J.; Zhao, Y. P. *Appl. Phys. Lett.* **2006**, *89*, 173134.

(30) (a) LeRu, E. C.; Blackie, E.; Meyer, M.; Etchegoin, P. G. *J. Phys. Chem. C* **2007**, *111*, 13794.

(31) (a) Wang, D. S.; Chew, H.; Kerker, M. *Appl. Opt.* **1980**, *19*, 2256–2257. (b) Kerker, M. *J. Colloid Interface Sci.* **1987**, *18*, 417–421.

(32) (a) Kneipp, K.; Kneipp, H.; Kneipp, J. *Acc. Chem. Res.* **2006**, *39*, 443–450. (b) Kneipp, K.; Kneipp, H.; Kartha, V. B.; Manoharan, R.; Deinum, G.; Itzkan, I.; Dasari, R. R.; Feld, M. S. *Phys. Rev. E* **1998**, *57* (6), R6281.

(33) (a) Jackson, J. B.; Halas, N. J. *Proc. Natl. Acad. Sci. U.S.A.* **2004**, *101*, 17930. (b) Jiang, J.; Bosnick, K.; Maillard, M.; Brus, L. *J. Phys. Chem. B* **2003**, *107*, 9964. (c) Gunnarsson, L.; Bjerneld, E. J.; Xu, H.; Petronis, S.; Kasemo, B.; Kall, M. *Appl. Phys. Lett.* **2001**, *78*, 802. (d) Nordlander, P.; Oubre, C.; Prodan, E.; Li, K.; Stockman, M. I. *Nano Lett.* **2004**, *4*, 899. (e) Pieczonka, N. P. W.; Aroca, R. F. *ChemPhysChem* **2005**, *6*, 2473. (f) Lee, S. J.; Morrill, A. R.; Moskovits, M. *J. Am. Chem. Soc.* **2006**, *128*, 2200.

(34) (a) Nie, S. M.; Emory, S. R. *Science* **1997**, *275*, 1102. (b) Michaels, A. M.; Nirmal, M.; Brus, L. E. *J. Am. Chem. Soc.* **1999**, *121*, 9932. (c) Krug, J. T.; Wang, G. D.; Emory, S. R.; Nie, S. M. *J. Am. Chem. Soc.* **1999**, *121*, 9208.

(35) Yguerabide, J.; Yguerabide, E. E. *Anal. Biochem.* **1998**, *262*, 137–156.

(36) (a) Kneipp, K.; Kneipp, H. *Isr. J. Chem.* **2006**, *46*, 299–305. (b) Thompson, D. G.; Enright, A.; Faulds, K.; Smith, W. E.; Graham, D. *Anal. Chem.* **2008**, *80*, 2805.

(37) Futamata, M.; Maruyama, Y.; Ishikawa, M. *J. Phys. Chem. B* **2003**, *107*, 7607.

(38) (a) Ren, B.; Lin, X. F.; Yang, Z. L.; Liu, G. K.; Aroca, R. F.; Mao, B. W.; Tian, Z. Q. *J. Am. Chem. Soc.* **2003**, *125*, 9598. (b) Cai, W. B.; Ren, B.; Li, X. Q.; She, C. X.; Liu, F. M.; Cai, X. W.; Tian, Z. Q. *Surf. Sci.* **1998**, *406*, 9. (c) Wang, Y. L.; Chen, H. J.; Dong, S. J.; Wang, E. K. *J. Chem. Phys.* **2006**, *125*, 044710.

(39) (a) Kao, P.; Malvadkar, N. A.; Cetinkaya, M.; Wang, H.; Allara, D. L.; Demirel, M. C. *Adv. Mater.* **2008**, *20*, 3562. (b) Sengupta, A.; Mujacic, M.; Davis, E. J. *Anal. Bioanal. Chem.* **2006**, *386*, 1379. (c) Laucks, M. L.; Sengupta, A.; Junge, K.; Davis, E. J.; Swanson, B. D. *Appl. Spectrosc.* **2005**, *59*, 1222. (d) Efrima, S.; Zeiri, L. *J. Raman Spectrosc.* **2009**, *40*, 277.

(40) (a) Williams, A. C.; Edwards, H. G. M. *J. Raman Spectrosc.* **1994**, *25*, 673. (b) Edwards, H. G. M.; Russell, N. C.; Weinstein, R.; Wynn-Williams, D. D. *J. Raman Spectrosc.* **1995**, *26*, 911. (c) Britton, K. A.; Dalterio, R. A.; Nelson, W. H.; Britt, D.; Sperry, J. F. *Appl. Spectrosc.* **1988**, *42*, 782. (d) Keir, R.; Sadler, D.; Smith, W. E. *Appl. Spectrosc.* **2002**, *56*, 551.

(41) Chu, H.; Huang, Y.; Zhao, Y. P. *Appl. Spectrosc.* **2008**, *62*, 922.

JP1015406